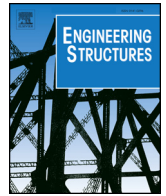


ELSEVIER

Contents lists available at ScienceDirect

Engineering Structures

journal homepage: www.elsevier.com/locate/engstruct

Effectiveness of dynamic vibration absorbers implemented in tall buildings

J.S. Love*, T.C. Haskett, B. Morava

RWDI, 600 Southgate Drive, Guelph, ON N1G 4P6, Canada

ARTICLE INFO

Keywords:

Structural monitoring
Tuned mass damper
Tuned sloshing damper
Structural control
Tall and super-tall buildings
Wind-induced motion
Inherent and effective damping

ABSTRACT

In recent decades, dynamic vibration absorbers (DVAs), such as tuned sloshing dampers (TSDs) and tuned mass dampers (TMDs) have been increasingly used to enhance the serviceability performance of tall buildings subjected to wind excitation. While the fundamental theory of ideal structure-DVA systems is well developed, there is a lack of available literature documenting the performance of DVA systems that have been installed in tall buildings. Moreover, it is challenging to directly quantify the effectiveness of DVAs installed in buildings due to the uncertainties associated with the applied wind loading. In particular, traditional methods are generally unable to directly calculate the effective damping that a DVA adds to the building.

This study presents the results of full-scale structural monitoring conducted on two tall buildings that have been equipped with DVAs to reduce wind-induced motion. The responses of the building and the DVA were monitored during significant wind events. The performance of the DVAs is directly determined by using the building and DVA responses, and the structure-DVA mass ratio, to calculate the added effective damping. The theoretical added effective damping of an ideal structure-DVA system is compared to the measured value, revealing that nonlinear effects that are typically neglected, such as friction, can significantly alter the theoretical added effective damping from its measured value at low response amplitudes. The DVAs studied have significantly decreased the wind-induced motions of the tall buildings monitored.

1. Introduction

The proliferation of tall and super-tall buildings in recent years has resulted in considerable challenges related to the performance of these structures when they are subjected to wind loading. While the lateral load resisting system of the building can be designed to resist the shear forces and overturning moments to which it is subjected during the ultimate design wind event, serviceability performance objectives during common wind events are often more challenging to achieve [1]. Without mitigation, sensitive occupants on the upper floors of the building may experience discomfort on windy days, as they are able to perceive the building motion. Moreover, the building motion may impact the performance of building partitions and decrease the longevity of facade components, thus increasing costs associated with building maintenance.

The low inherent structural damping associated with most tall buildings is one of the main contributors to their susceptibility to wind-induced motions. To reduce building motion during common wind events, supplementary damping systems, such as dynamic vibration absorbers (DVAs) have become increasingly popular [2]. Two common types of DVAs are the tuned mass damper (TMD) and the tuned sloshing

damper (TSD), also known as the tuned liquid damper (TLD). These devices are often modeled as auxiliary spring-mass-dashpot systems that are coupled to the primary structure. As the building experiences a resonant response, a properly designed DVA will interact with the structure, altering its mechanical admittance function, and leading to a decreased response. McNamara [3] derived the frequency-response function and the effective damping of a structure-DVA system subjected to white noise excitation, which is now commonly used to model wind loading.

The performance of a DVA is typically quantified using the concept of effective damping [4]. The effective damping may be understood as the amount of damping that the bare structure (without a DVA) must possess to experience the same response variance as the structure equipped with the DVA. Mathematically, the effective damping for the structural mode being controlled may be expressed as:

$$\zeta_{eff} = \zeta_{str} \frac{\sigma_{str}^2}{\sigma_{str-damped}^2} \quad (1)$$

where ζ_{str} is the inherent structural damping, σ_{str} is the root-mean-square (RMS) response of the structure without a DVA, and $\sigma_{str-damped}$ is the RMS response of the structure equipped with a DVA. Alternatively,

* Corresponding author.

E-mail address: Shayne.Love@rwdi.com (J.S. Love).

if the mechanical admittance function of the structure equipped with a DVA, $H_{str-damped}(\omega)$ is known, the effective damping may be calculated as [4]:

$$\zeta_{eff} = \frac{\pi}{4} \omega_{str} \left[\int_0^\infty |H_{str-damped}(\omega)|^2 d\omega \right]^{-1} \quad (2)$$

where ω_{str} is the natural angular frequency of the structure. The amount of effective damping that a DVA appears to add to a structure (the “added effective damping”) is quantified as:

$$\zeta_{added} = \zeta_{eff} - \zeta_{str} \quad (3)$$

When a DVA is installed in an actual tall building, it has traditionally been challenging to verify its performance by calculating its effective damping or added effective damping. Equation (1) requires knowledge of both the building response with and without a DVA ($\sigma_{str-damped}$ and σ_{str}), which cannot be measured simultaneously. Tamura et al. [5] inferred the structural responses and performance with and without a DVA by conducting long term structural monitoring, but in many cases this is undesirable due to the associated costs and desire to avoid subjecting occupants to the undamped building response. Alternatively, Eq. (2) requires knowledge of the mechanical admittance function of the building equipped with a DVA. Since the external excitation is generally not known, it is difficult to calculate the mechanical admittance function from a measured response. It is possible to reconstruct the theoretical mechanical admittance function if the dynamic properties (mass, stiffness, and damping) of the building and DVA are known; however, it is often challenging to identify the properties of coupled systems from ambient vibration measurements [6,7]. Moreover, this type of system identification methodology is quite complicated, and it would be beneficial if a more practical method to predict the added effective damping produced by a DVA were available.

Love and Tait [8] recently proposed a simple method to estimate the added effective damping of nonlinear structure-DVA systems when the structure is subjected to white noise random excitation. The method provides a direct calculation of the added effective damping based on the DVA-structure mass ratio and the responses of the structure and DVA(s). It was found to provide satisfactory results when evaluated using nonlinear simulations, as well as scale-model testing on a structure-TSD system. The benefit of this method is that it enables the performance of the DVA to be evaluated without using long-term monitoring with and without the DVA installed as was done in Ref. [5], nor does it require the dynamic properties of the system to be estimated using sophisticated system identification algorithms (such as Ref. [9]) to reconstruct the theoretical mechanical admittance function of the structure.

The purpose of the current study is two-fold. Firstly, it seeks to evaluate the model proposed by Love and Tait [8] using data collected from full-scale structural monitoring of two tall buildings equipped with DVAs. Its predictions are compared to the theoretical level of added effective damping using the estimated properties of the building and DVA. Secondly, the study seeks to evaluate the performance of the full-scale DVAs considered, to confirm that the devices are providing significant acceleration reductions. The first building is 10 Barclay Street in New York City, which is equipped with a unidirectional TSD. The second building studied is an anonymous super-tall slender tower that is equipped with two bi-directional TMDs.

2. Background

2.1. Structure-DVA system

If the directions of motion of the two structural sway modes are perpendicular, and the DVA direction of motion is aligned with the structural mode it is controlling, the structure-DVA system may be represented as shown in Fig. 1. A total of n DVAs with nonlinear damping may be tuned to a single structural mode. In Fig. 1, M_{str} , ω_{str} , and ζ_{str} are

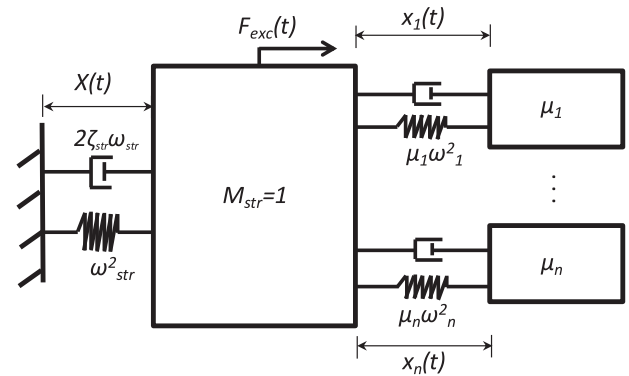


Fig. 1. Model of structure equipped with multiple DVAs.

the generalized mass, natural angular frequency, and damping ratio of the structure, respectively, while ω_i and ζ_i are the natural frequency and damping ratio of the i th DVA, respectively. When the damping force of the DVA is nonlinear, statistical linearization techniques are employed to represent the damping ratio as amplitude-dependent equivalent viscous damping [10]. The external force applied to the structure is $F_{exc}(t)$, displacement response of the structure is $X(t)$, and the relative displacement between the structure and the i th DVA is $x_i(t)$. The equations of motion for the structure and the i th DVA mass are:

$$\left(1 + \sum_{i=1}^n \mu_i \right) \ddot{X}(t) + \sum_{i=1}^n \mu_i \ddot{x}_i(t) + 2\omega_{str}\zeta_{str}\dot{X}(t) + \omega_{str}^2 X(t) = F_{exc}(t) \quad (4)$$

$$\ddot{x}_i(t) + 2\omega_i\zeta_i\dot{x}_i(t) + \omega_i^2 x_i(t) = -\ddot{X}(t) \quad (5)$$

where each dot above a variable denotes a time derivative. If the structure-DVA system is bi-directional, another independent set of equations, and a corresponding set of dynamic properties exist for the perpendicular direction. In this study, the properties in the X- and Y-directions will be distinguished (when necessary) using the subscripts X and Y, respectively. The natural cyclic frequency, f (in units of Hz) is related to the angular frequency by $\omega = 2\pi f$. The solution to the equations of motion is straightforward, but tedious, and can be found elsewhere [3,11].

In this study, TSDs are represented as equivalent mechanical systems using well-known formulae for sloshing in a rectangular tank [12]. The tank has a length, L , width, b , and quiescent water depth, h , and is equipped with screens to increase the liquid damping. When screens are present in deepwater TSDs, they can be represented as an equivalent mechanical system, and have been shown to be effective in reducing building motion [12].

2.2. Added effective damping estimation

For structures subjected to white noise excitation, the mean rate of energy input into the system (that is, the mean power) depends only upon the excitation amplitude and the mass of the structure [13]. Therefore, for a stationary system, the mean power input and output for the system does not change when a DVA is coupled to the structure. By making use of this property, it has been shown that the added effective damping produced by a DVA can be calculated as [8]:

$$\zeta_{added} = \frac{\omega_{str} \sum_{i=1}^n \mu_i E[\dot{X}(t)\dot{x}_i(t)]}{2\sigma_{\ddot{X}-damped}^2} \quad (6)$$

where $\sigma_{\ddot{X}-damped}^2$ is the variance of the structural acceleration, and $E[\dot{X}(t)\dot{x}_i(t)]$ represents the covariance between the structural acceleration and the DVA relative velocity. Since the response of the structure and DVA are measured, only the DVA-structure mass ratio and natural angular frequency of the structure need to be estimated. In most cases, the mass ratio is known with reasonable accuracy, and if the as-

built natural angular frequency of the structure is unknown, it can be estimated as a weighted average of the measured acceleration spectrum, $S_{\ddot{x}-damped}(\omega)$:

$$\omega_{str} \cong \frac{\int_0^\infty \omega S_{\ddot{x}-damped}(\omega) d\omega}{\sigma_{\ddot{x}-damped}^2} \quad (7)$$

This method of determining the added effective damping has been evaluated using numerical simulations and scale-model structure-TSD testing, and was found to produce acceptable results [8]. In this study, the methodology is further evaluated using full-scale structural monitoring data.

3. Full-scale structural monitoring

This section presents structural monitoring results of one tall and one super-tall building equipped with DVAs when they each experienced significant wind events. Note that in the following sections, the unit of milli-g is used, where 1 milli-g is defined as one-thousandth of gravitational acceleration. In the response spectra presented, the frequency axis is normalized by the first structural frequency, while the magnitude of the power spectrum is normalized by the variance of the response plotted. The analysis conducted in the following sections assumes that the wind loading can be represented as white noise excitation; an assumption often employed in wind engineering to greatly simplify the analysis without sacrificing the accuracy. Moreover, for the theoretical structure-DVA modelling, the structure is assumed to be linear and the TMD is assumed to possess no friction.

3.1. Tall building #1: 10 Barclay Street

3.1.1. Background

The first tall building monitored is 10 Barclay Street, located in Lower Manhattan, USA. The structure has a height of 204 m, and typical floor plate dimensions of 19.5 m × 45.4 m, yielding a slenderness ratio of 10.5 [14]. A TSD system was installed to provide 1.5% added effective damping to the first structural vibration mode to reduce the anticipated peak hourly acceleration from 23 milli-g to less than 18 milli-g at the 10-year mean recurrence interval wind event. An inherent structural damping ratio of 2% was assumed at the 10-year mean recurrence interval wind event, although less damping is expected at smaller building responses. Structural motion along the shorter building direction dominates the response, therefore only one mode requires supplemental damping.

The TSD is unidirectional with plan dimensions of 13.72 m × 5.49 m, and a quiescent water depth of 1.98 m. The natural sloshing frequency of the TSD is therefore 0.97 rad/s, and its equivalent mechanical mass is 113 tonnes (75% of the total water mass), which resulted in a DVA-structure mass ratio of approximately 0.9%. Three screens were positioned at 25%, 50%, and 75% of the tank length to increase the TSD damping. The effective solidity ratio of the screens was approximately 41%, which produces a loss coefficient of $C_l = 1.96$ according to empirical relationships [15]. Table 1 summarizes the

Table 1
Dynamic properties of Building #1.

Property	Value
ω_{str}	0.97 rad/s
ζ_{str}	1%
μ	0.9%
L	13.72 m
b	5.49 m
h	1.98 m
x_j/L	25%, 50%, 75%
C_l	1.96

pertinent properties of the structure-TSD system.

3.1.2. Structural monitoring

Structural monitoring of the building was conducted during a significant wind event that occurred February 19–20, 2011. During the wind event, the response of the structure was recorded using accelerometers that were temporarily installed at the top of the building. While the accelerometers monitored motion in both principal building directions, for brevity only the response in the dominant direction is presented herein. TSD wave heights at the tank end wall were recorded using an ultrasonic wave probe that was mounted through the tank ceiling. Sampling was conducted at 25 Hz, with a low pass filter applied at 3.7 Hz.

3.1.3. Temporal response

The wave heights are converted to the displacements of an equivalent mechanical system [12]. The wave heights are low pass filtered to remove the contribution of the higher order sloshing modes, which are present in the fluid response due to the nonlinear coupling of the sloshing modes [16]. Fig. 2 shows a 4000 s record of building acceleration and the TSD wave heights, which corresponds to the time when the building response is most significant. Fig. 2 also shows an enlarged segment of that record, in which the effect of filtering the wave heights to remove the higher order modes is visible. Removal of the higher sloshing modes decreases the height of the wave peaks, and increases the depth of the troughs, since the higher sloshing modes are responding at frequencies that are approximately integer multiples of the fundamental mode [16]. The peak observed building acceleration is 5.7 milli-g, while the peak unfiltered wave height is 0.36 m.

3.1.4. Spectral response

Fig. 3 shows normalized response spectra of building accelerations and the TSD wave heights presented in Fig. 2. The RMS response of the building and filtered TSD wave heights are 1.26 milli-g and 0.074 m, respectively. Using the TSD model presented earlier and the system properties shown in Table 1, the magnitude of the white noise excitation, S_0 can be adjusted to match the RMS structural acceleration of 1.26 milli-g. At this excitation magnitude, the predicted RMS sloshing response is 0.062 m, which corresponds to a 15% relative error with the monitoring results.

3.1.5. Added effective damping

The added effective damping is calculated from the measured structural and TSD responses using Eq. (6). Using the 4000-second segment of data shown in Fig. 2, the added effective damping is calculated to be 2.04%. Using the TSD model, the theoretical added effective damping is 1.72%, which corresponds to a relative error of 15%. For the TSD model calculations, an inherent structural damping ratio of 1% has been assumed, since at these low response levels, it is not expected that 2% inherent structural damping will be achieved. If 2% inherent structural damping is assumed, the theoretical added effective damping decreases slightly to 1.59%. There is uncertainty in the inherent structural damping, since it cannot be directly determined from the measurements of the coupled structure-TSD system.

While the wind event measured was significant, it was much less intense than the 10-year mean recurrence interval wind event. For this reason, the damping in the TSD was less than optimal, resulting in reduced TSD performance. Despite this, the measurements indicated that the TSD provided added effective damping of 2.04%, which exceeded the originally desired added effective damping of 1.5%. Using Eq. (1), and assuming an inherent structural damping ratio of 1%, the TSD is estimated to have reduced the RMS building acceleration by 43%.

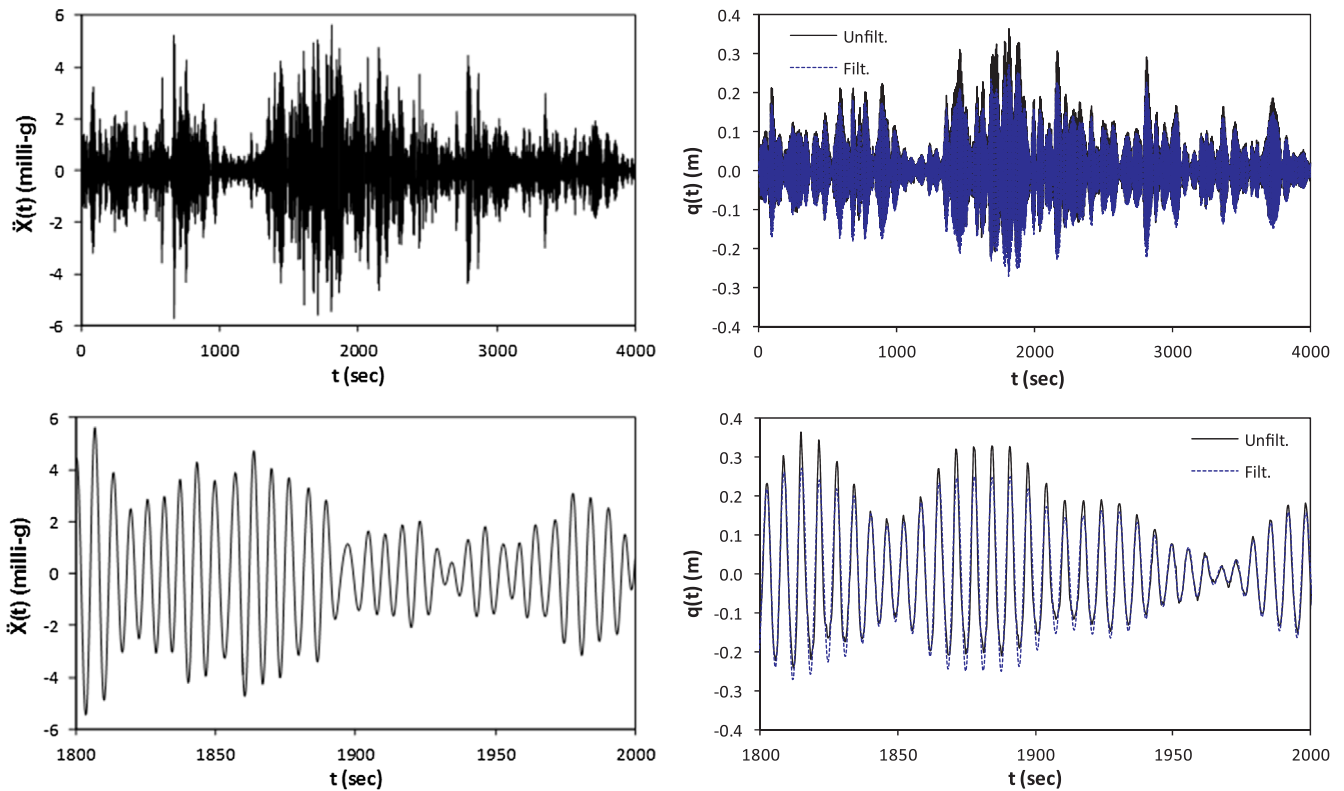


Fig. 2. Building #1 acceleration and TSD wave heights (top) 4000-second record, (bottom) 200-second segment.

3.2. Tall building #2

3.2.1. Background

The second building studied is an anonymous super-tall tower. Wind tunnel tests indicated that the first two modes of vibration were susceptible to excessive wind-induced motion during common wind events. To reduce these motions, two identical bi-directional TMDs weighing several hundred tonnes were installed in the building. These two TMD masses result in a total TMD-structure mass ratio of 4.4%. Since the building frequencies were expected to be similar, and the TMD mass ratio was large, the TMDs were designed to have identical frequencies in both directions, without resulting in any significant loss of performance. This identical tuning enabled the expense of a bi-tuning mechanism to be avoided. As a result of this identical tuning, the TMD is tuned to a slightly lower than optimal frequency in the X-direction, while it is tuned to a slightly higher than optimal frequency in the Y-direction.

The TMDs employ velocity-squared damping to help control TMD

Table 2

Dynamic properties of Building #2.

Property	X-direction	Y-direction
ω_{str}	0.54 rad/s	0.52 rad/s
ζ_{str}	0.6%	0.6%
μ	4.4%	4.4%
$\omega_{DVA}/\omega_{str}$	96.8%	99.6%
α	2	2
c_0	1580 kN * (s/m) ²	624 kN * (s/m) ²

displacements during very strong wind events. Due to the local wind climate and surrounding buildings, the structure is expected to be livelier in the Y-direction, therefore the damping coefficients in the two directions are dissimilar. Table 2 provides a summary of the dynamic properties of the structure-TMD system. Prior to the TMDs being commissioned, measurements were conducted to determine the building's dynamic properties without the effects of the coupled TMDs, as

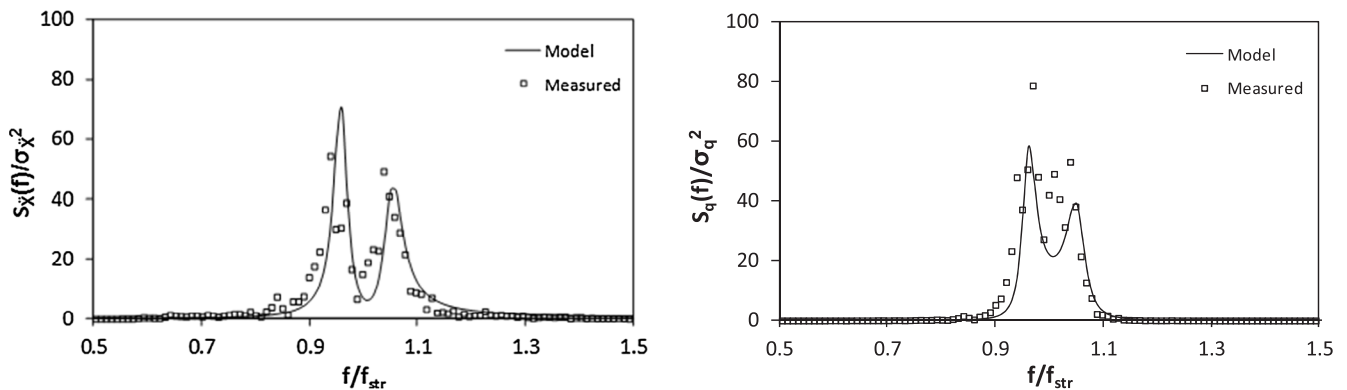


Fig. 3. Building # 1 normalized response spectra of acceleration and TSD wave heights.

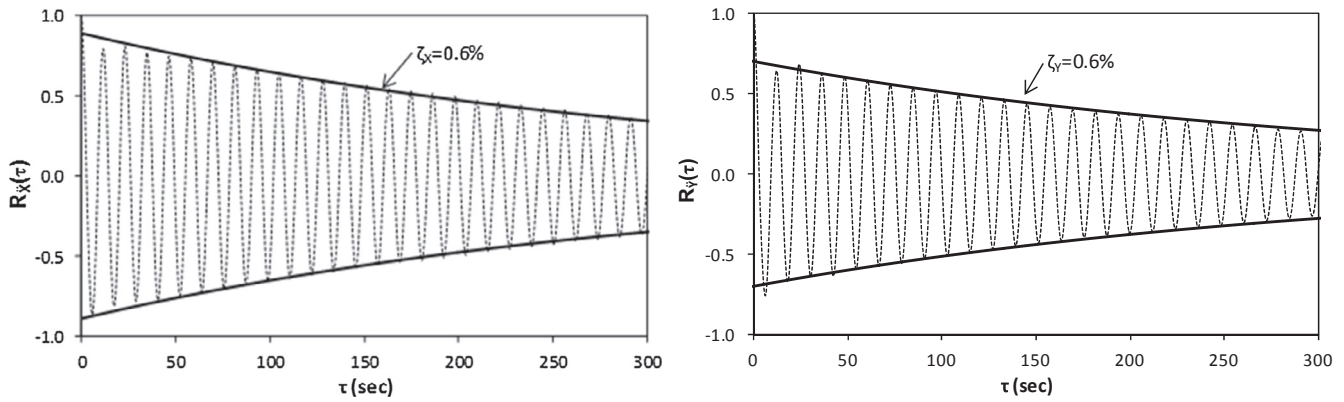


Fig. 4. Building #2 normalized random decrement signature of building with TMDs locked-out.

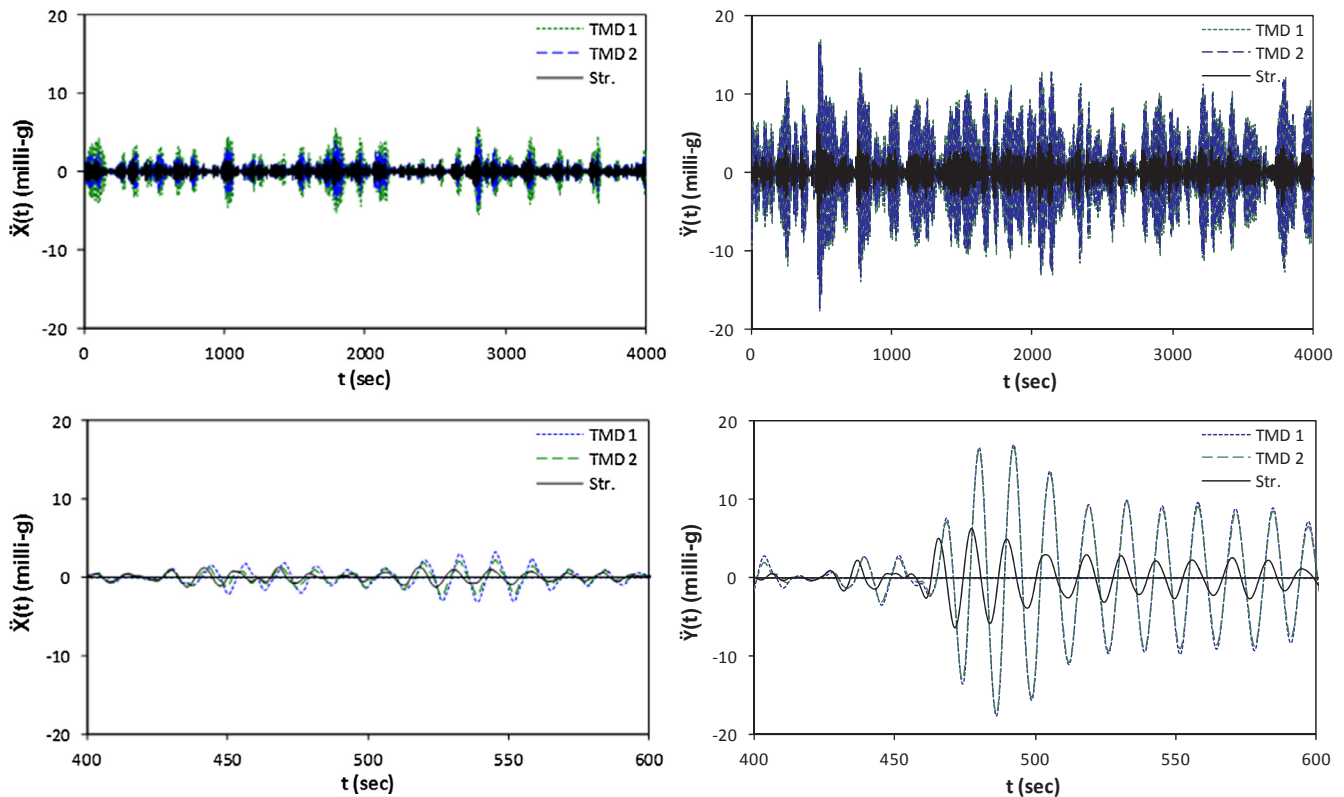


Fig. 5. Building #2 accelerations of building and TMDs (top) 4000-second record, (bottom) 200-second segment (Nov. 2016 wind event).

described in the next section.

3.2.2. Structural monitoring

The building was monitored for approximately one day while the TMDs were locked-out, which enabled the properties of the bare structure to be estimated at low levels of ambient excitation. After correcting for the additional inertial mass of the locked-out TMDs, the natural sway frequencies are estimated to be 0.54 rad/s and 0.52 rad/s in the X- and Y-directions, respectively. The inherent structural damping of the building was estimated using the random decrement technique [17]. Fig. 4 shows the random decrement signature generated using the autocorrelation of the ambient vibration response. The response envelope created by assuming a 0.6% damping ratio is a good fit to the random decrement signatures of the tower in the X- and Y-directions.

After the TMDs were commissioned, four bidirectional accelerometers were left installed at the top of the building. Two of these accelerometers were installed on the building in opposing corners,

while the remaining two accelerometers were installed on each TMD mass. The acceleration of the building in the X- and Y-directions is determined by averaging the two accelerometers attached to the building.

3.2.3. Temporal response

Fig. 5 shows a 4000-second record of the building and TMD accelerations in the X- and Y-directions during a significant wind event that occurred in November 2016. Also shown is a 200-second enlarged segment of that record. The peak building acceleration in the X-direction is approximately 2.2 milli-g, while the peak response observed in the Y-direction is approximately 6.4 milli-g. The acceleration response of the TMDs is much larger, with peak accelerations of approximately 6 milli-g and 17 milli-g in the X- and Y-directions, respectively. As a result of the low accelerations in the X-direction, mechanical friction within the TMDs is more likely to appreciably influence the TMD response in the X-direction. For the first few response cycles of the enlarged segment in Fig. 5, the absolute TMD and building accelerations are

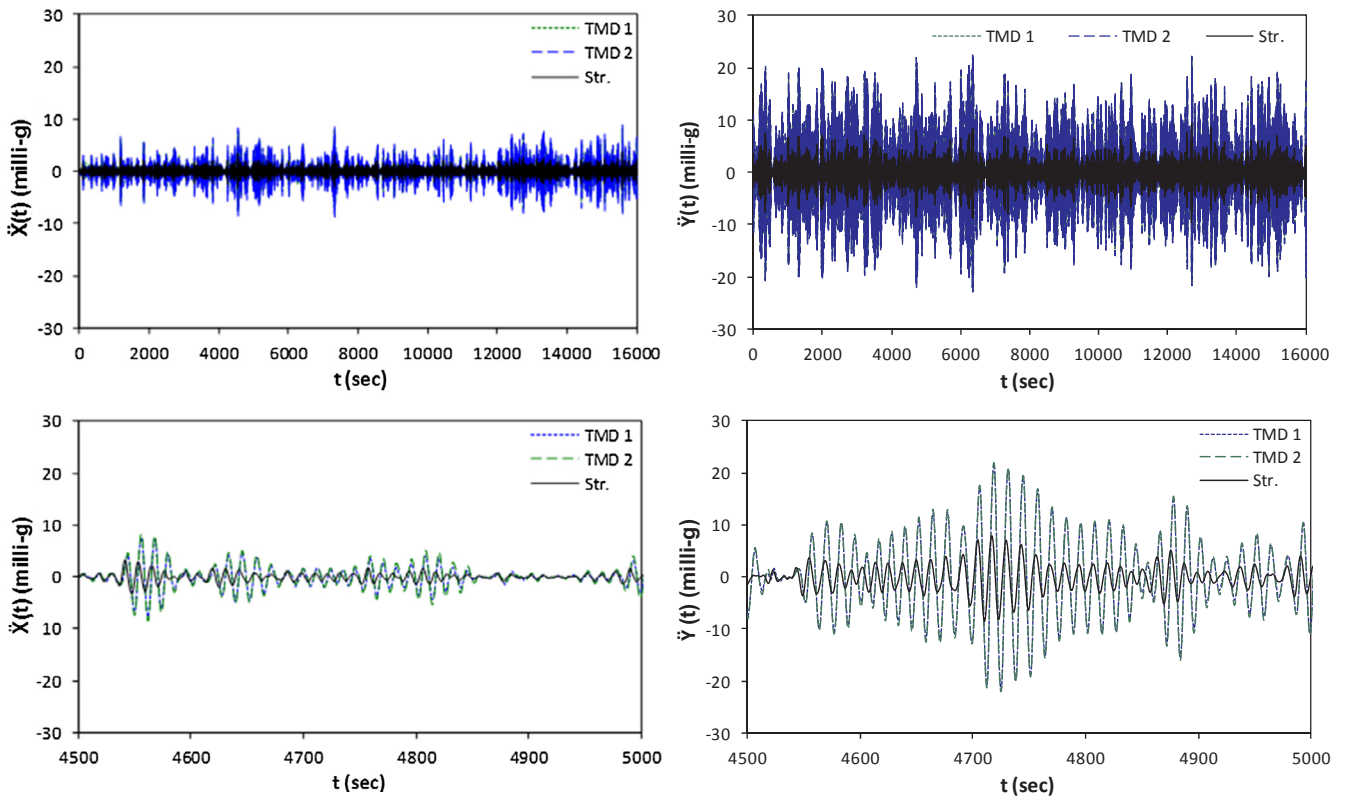


Fig. 6. Building #2 accelerations of building and TMDs (top) 16,000-second record, (bottom) 500-second segment (Feb. 2017 wind event).

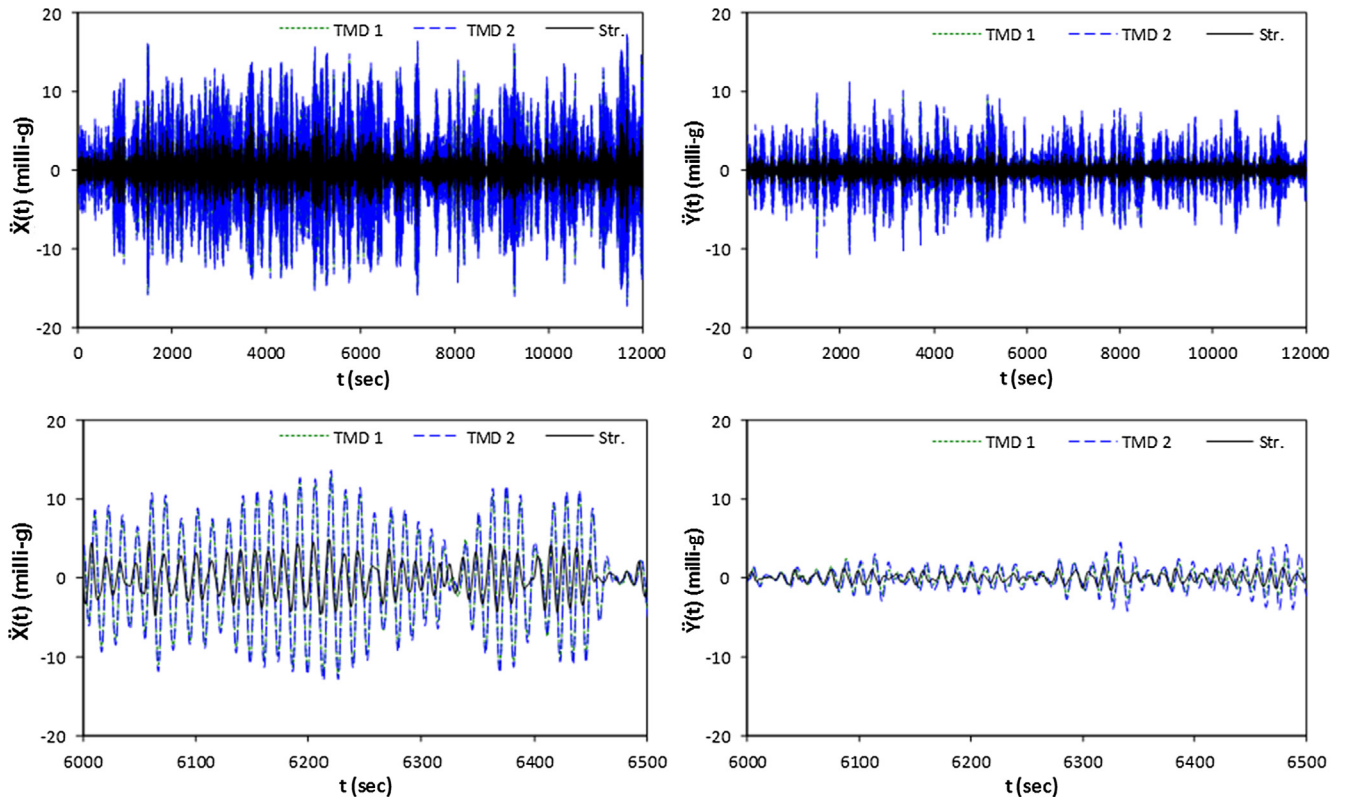


Fig. 7. Building #2 accelerations of building and TMDs (top) 12,000-second record, (bottom) 500-second segment (Mar. 2017 wind event).

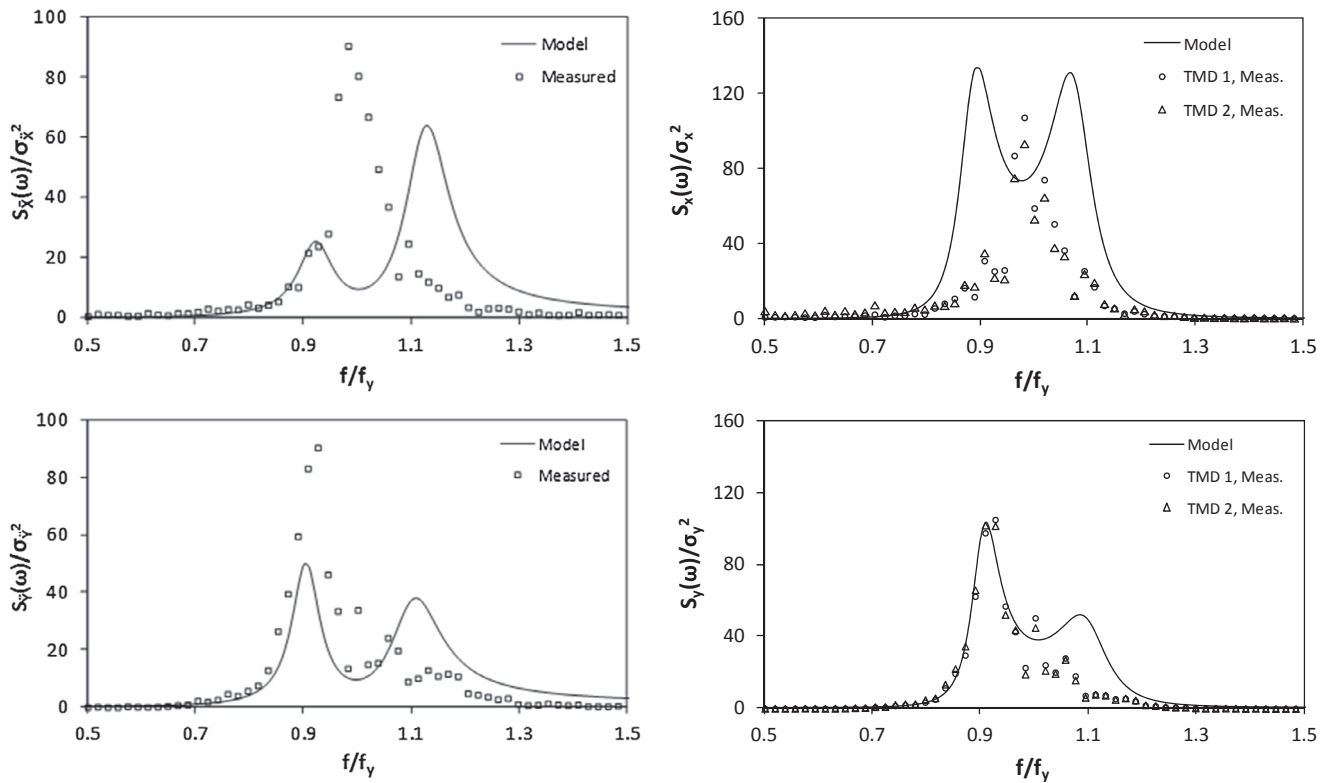


Fig. 8. Building #2 spectral accelerations and TMD relative displacements (top) X-direction, (bottom) Y-direction (Nov. 2016 wind event).

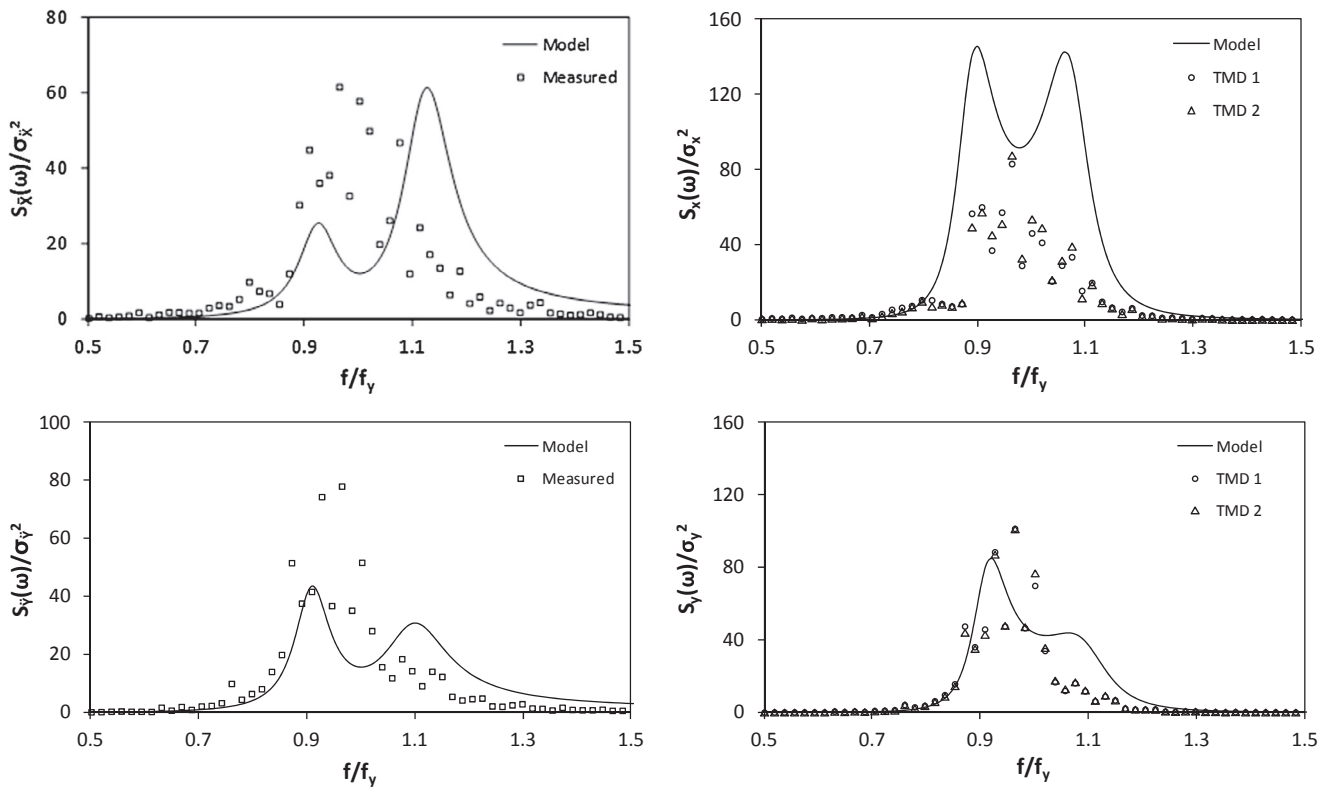


Fig. 9. Building #2 spectral accelerations and TMD relative displacements (top) X-direction, (bottom) Y-direction (Feb. 2017 wind event).

identical, indicating that the TMDs are moving rigidly with the building (they have not yet overcome the weak mechanical friction forces). The measurements reveal that the TMDs overcome the friction forces when the building acceleration exceeds approximately 0.5–1.0 milli-g.

Therefore, the TMDs begin to function at building accelerations that are well below the threshold of human perception [18]. Fig. 5 also shows that the two TMDs have a noticeably different response in the X-direction. This trend is expected to be a result of minor differences in the

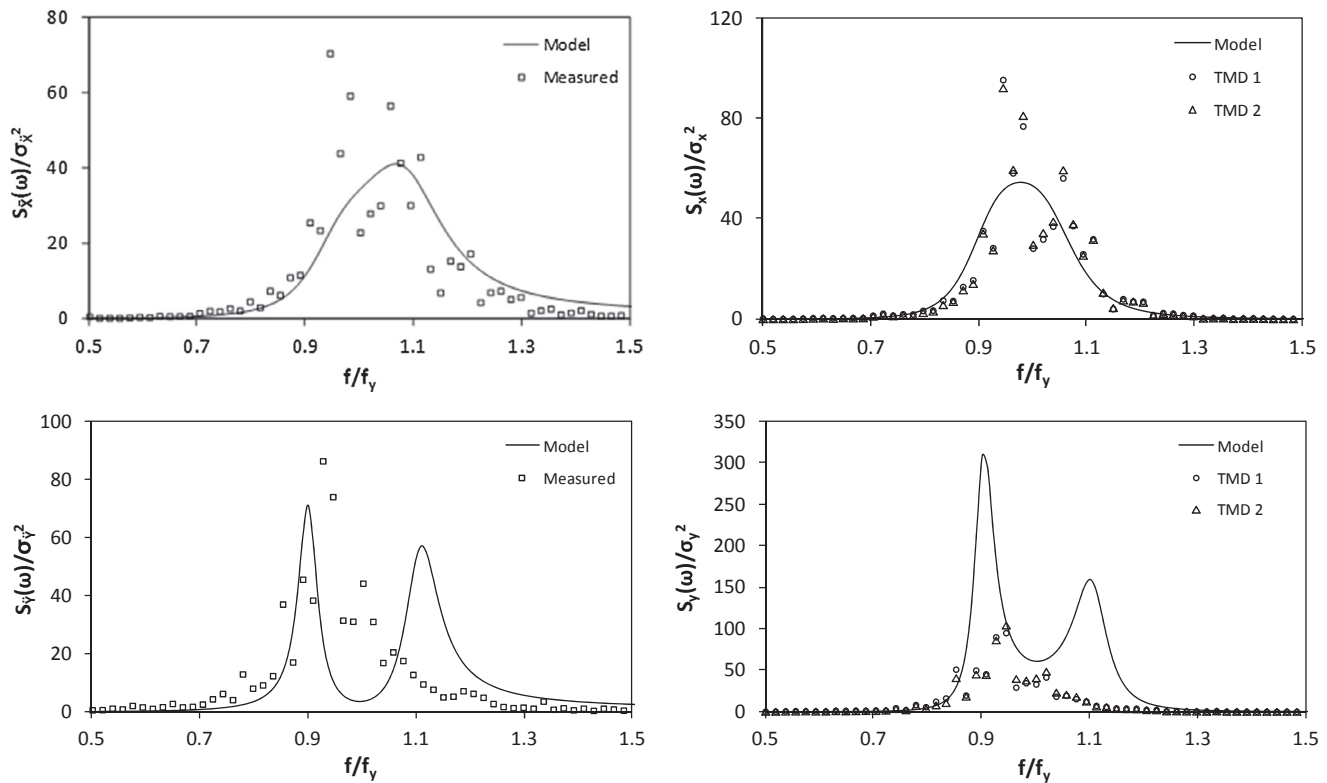


Fig. 10. Building #2 spectral accelerations and TMD relative displacements (top) X-direction, (bottom) Y-direction (Mar. 2017 wind event).

Table 3
Measured and predicted RMS responses of Building #2.

Direction	Response	Unit	Nov. 2016	Feb. 2017	Mar. 2017
X	Meas. Building Accel.	(milli-g)	0.59	0.70	1.85
	Meas. TMD 1 Disp.	(m)	0.048	0.052	0.162
	Meas. TMD 2 Disp.	(m)	0.027	0.067	0.178
	Pred. TMD Disp.	(m)	0.076	0.084	0.159
Y	Meas. Building Accel.	(milli-g)	1.41	2.06	0.82
	Meas. TMD 1 Disp.	(m)	0.165	0.219	0.066
	Meas. TMD 2 Disp.	(m)	0.149	0.228	0.088
	Pred. TMD Disp.	(m)	0.191	0.246	0.125

Table 4
Measured and predicted added effective damping for Building #2.

Direction		Nov. 2016	Feb. 2017	Mar. 2017
X	Modeled	4.9%	5.0%	4.6%
	Measured	3.0%	4.1%	5.1%
Y	Modeled	4.8%	5.0%	4.0%
	Measured	5.0%	4.7%	4.1%

amount of friction in the two TMDs. As the response amplitude increases, the effects of friction will become less noticeable, and it is expected that the response of the two TMDs will converge. In the Y-direction, where the response amplitude is much larger, the response of the two TMDs is nearly identical, since the effects of friction are insignificant when compared to the other dynamic forces acting on the system.

Building and TMD accelerations from two additional wind events that occurred in February and March of 2017 are shown in Figs. 6 and 7, respectively. These figures show the portion of the wind event that resulted in significant accelerations over a period of several hours. The peak building accelerations recorded during the February 2017 event

were 3.4 milli-g and 8.6 milli-g in the X- and Y-directions, respectively. The peak building accelerations recorded during the March 2017 event were 8.2 milli-g and 4.0 milli-g in the X- and Y-directions, respectively. The March 2017 event was particularly rare, as the building motion in the X-direction was greater than the Y-direction due to the direction of the wind. In this case, the TMD in the X-direction experiences significant motion, while the TMD in the Y-direction is observed to often be locked-out due to friction.

3.2.4. Spectral response

Figs. 8–10 show the normalized response spectra for the building acceleration and TMD relative displacements for the X- and Y-directions, respectively for the November 2016, February 2017, and March 2017 wind events, respectively. Both the measured responses and the responses predicted from the system properties are shown. The predicted response is calculated by determining the magnitude of the white noise excitation, S_0 that will produce the measured RMS building accelerations for each direction. The measured RMS building accelerations as well as the measured and predicted TMD relative displacements are summarized in Table 3.

In Table 3, considerable discrepancies exist between the predicted and measured responses of the TMDs when building acceleration in that direction is low. For example, from Table 3 the X-direction TMD relative displacement measured during the November 2016 wind event were 40–60% less than was predicted. A similar trend is observed in the X-direction during the February 2017 event, and in the Y-direction during the March 2017 event. In all these cases, the RMS building acceleration was less than 1 milli-g. Conversely, when the RMS building accelerations exceeded 1.4 milli-g, the relative error between the measured and predicted TMD relative displacements is less than 25%. The trend of larger discrepancies at low excitation levels is also observed in the response spectra of Figs. 8–10. The model predicts double-peaked building and TMD response spectra under low excitation levels; however the measurements reveal a single broad peak when the associated RMS building acceleration is less than 1 milli-g. Better agreement

between the model and measurements is observed when the response increases, although discrepancies are still present.

The discrepancies between the predicted and measured relative TMD displacements during low excitation levels are largely attributed to friction, which locks-out the TMDs during periods of time when building accelerations are less than approximately 1 milli-g. The differences between the modeled and measured results when the excitation is large may be a result of nonlinear effects from the structure, and the mechanical friction may still influence the response somewhat. The exact cause of the discrepancies is not easily ascertained from measurements conducted, and is beyond the current scope of work. Despite the friction and model discrepancies, it will be shown in the next section that the TMDs are providing considerable acceleration reduction.

3.2.5. Added effective damping

The added effective damping is calculated from the measured building and TMD responses using Eq. (6). Table 4 summarizes the added effective damping that is theoretically predicted using the TMD model and the measured one which is estimated based on Eq. (6). The theoretical added effective damping predicted by the model is generally 4–5% depending on the building response amplitude. The measured added effective damping is generally between 4% and 5%, with the exception of the X-direction during the November 2016 event. During this event, the measured added effective damping was only 3% due to the TMD being locked-out by friction at low building accelerations. With the exception of the X-direction during the November 2016 and February 2017 events, the measured and predicted added effective damping show relative errors of less than 10%. Using Eq. (1) and assuming the inherent structural damping ratio remains 0.6% at these response amplitudes, the TMDs are reducing the RMS building accelerations by 59–67% in both directions. Therefore, despite discrepancies between the predicted and measured response spectra, the TMDs are providing considerable acceleration reductions during these wind events.

4. Conclusions

There are currently few studies available that have evaluated the performance of structure-DVA systems using full-scale structural monitoring. In this study, results have been presented from structural monitoring conducted on two tall buildings equipped with a TSD or TMD system to reduce wind-induced motions. The added effective damping provided by the DVAs has been quantified using a recently developed technique.

Structural monitoring results from two tall buildings equipped with TMD or TSD systems were presented. The first tall building is equipped with a unidirectional TSD. The monitoring results indicated that during the wind event recorded, the TSD was providing 2.04% added effective damping to the building, which reduced building accelerations by approximately 43%. This level of added effective damping was in agreement with the theoretical predictions.

The second building studied was an anonymous super-tall building equipped with two identical bi-directional TMDs. Structural monitoring conducted while the TMDs were locked-out enabled the building frequencies and inherent structural damping ratios to be estimated. The structural monitoring indicated that at imperceptible building accelerations (< 1 milli-g), friction in the TMDs causes them to periodically lock-out. This nonlinear behaviour produces discrepancies with the theoretical spectral responses. However, during the notable wind events reported, the TMDs still provided 4–5% added effective damping, which reduced accelerations by 59–67%. The measured added effective damping was in agreement with theoretical predictions.

The results of this study have demonstrated that the full-scale structure-DVA systems monitored are performing as intended, and the DVAs studied have considerably reduced the wind-induced motions of the tall buildings monitored. Nonlinear effects, such as friction, appear to have a small impact on device performance during wind events of interest. For the first time reported in the literature, a practical method has been employed to directly quantify the added effective damping of tall buildings equipped with DVAs using full-scale measurements.

References

- [1] Tamboli A. Tall and supertall buildings: planning and design. New York: McGraw-Hill Education; 2014.
- [2] Soto M, Adeli H. Tuned mass dampers. Arch Comput Methods Eng 2013;20(4):419–31.
- [3] McNamara R. Tuned mass dampers for buildings. J Struct Div 1977;ST9:1785–98.
- [4] Vickery B, Davenport A. An investigation of the behaviour in wind of the proposed Centrepoint Tower. Research Report – Boundary Layer Wind Tunnel (BLWT)-1-70, London, ON, Canada; 1972.
- [5] Tamura Y, Fujii K, Ohtsuki T, Wakahara T, Kohsaka R. Effectiveness of tuned liquid dampers under wind excitation. Eng Struct 1995;17(9):609–21.
- [6] Hazra B, Sadhu A, Lourenco R, Narasimhan S. Re-tuning tuned mass dampers using ambient vibration measurements. Smart Mater Struct 2010;19:115002.
- [7] Tamura Y, Yoshida A, Zhang L. Evaluation techniques for damping in buildings. In: International workshop on wind engineering & science, New Delhi; 2004.
- [8] Love J, Tait M. Estimating the added effective damping of SDOF systems incorporating multiple dynamic vibration absorbers with nonlinear damping. Eng Struct 2017;130:154–61.
- [9] Lin CC, Wang J, Ueng J. Vibration control identification of seismically excited MDOF structure-PTMD systems. J Sound Vib 2001;240(1):87–115.
- [10] Rudinger F. Tuned mass damper with nonlinear viscous damping. J Sound Vib 2007;300:932–48.
- [11] Kareem A, Kline S. Performance of multiple mass dampers under random loading. J Struct Eng 1995;121(2):348–61.
- [12] Tait M. Modelling and preliminary design of a structure-TLD system. Eng Struct 2008;30:2644–55.
- [13] Newland D. Calculation of power flow between coupled oscillators. J Sound Vib 1966;3(3):262–76.
- [14] Morava B, Alkhatib R, Grossman J, Klein G, Han S. Tuned sloshing damper for wind-induced motion control of a tall residential tower. In: ASCE structures congress, Orlando, FL; 2010.
- [15] Tait M, El Damatty A, Isyumov N, Siddique M. Numerical flow models to simulate tuned liquid dampers (TLD) with slat screens. J Fluids Struct 2005;20:1007–23.
- [16] Faltnsen O, Timokha A. Sloshing. Cambridge: Cambridge University Press; 2009.
- [17] Asmussen J, Ibrahim S, Brincker R. Random decrement: identification of structures subjected to ambient excitation. p. 914–21.
- [18] Architectural Institute of Japan Recommendations. Guidelines for the evaluation of habitability to building vibration. Tokyo, Japan; 2004.